Supplementary Material, Methods and Results

INDEX

Supplementary Material, Methods and Results 1
MRI data acquisition and quality check 2
16p11.2 European Consortium 2
Simons VIP study 3
Brain Canada 3
UCLA 4
Cardiff 4
MRI quality control 5
List of abbreviations 5
eMethod 1: MRI data processing, Voxel-Based Morphometry 5
eMethod 2: MRI data processing, Surface-Based Morphometry 6
eMethod 3: Multi-view pattern-learning analysis 6
eMethod 4: Voxel-based measures and statistical analyses 7
eMethod 5: Spin permutation testing 8
eMethod 6: Label shuffling 8
eTable 1 : Demographics 9
eTable 2 : CNV effect sizes on local grey matter volume changes. 10
eTable 3: CNV effect sizes on local Surface Area changes. 11
eTable 4: CNV effect sizes on local Cortical Thickness changes. 12
eTable 5: Canonical Correlation Analysis ROIs loadings. 13
eTable 6: Canonical Correlation Analysis ROIs loadings (CT). 14
eTable 7: Canonical Correlation Analysis ROIs loadings (SA). 15
eTable 8: Brain-wide Cohen's d map Correlations for VBM 16
eTable 9: Cortex-wide Cohen's d map Correlations for SA 16
eTable 10: Cortex-wide Cohen's d map Correlations for CT 17
eTable 11: Within loci comparison of Cohen's d variances between deletions and duplications. 18
eFigure 1: CCA analysis across 4 CNVs Cortical Thickness. 19
eFigure 2: CCA analysis across 4 CNVs Surface Area. 21
eFigure 3: FDR corrected Cohen's d maps of Surface Area. 22
eFigure 4: FDR corrected Cohen's d maps of Cortical Thickness. 23
eFigure 5: Spatial overlap across duplications at 3 and 4 genomic loci 25
eFigure 6: Spatial overlap for surface area (SA) across deletions. 26

eFigure 7: Spatial overlap for surface area (SA) across duplications. 28
eFigure 8: Spatial overlap for mean cortical thickness (CT) across deletions. 29
eFigure 9: Spatial overlap for mean cortical thickness (CT) across duplications. 30
eFigure 10: Comparison of convergence patterns across brain measures. 32
eFigure 11: Dice indices between cross-psychiatric disorder map and CNVs convergence patterns. 33

MRI data acquisition and quality check

16p11.2 European Consortium

MRI data of the EU participants were acquired on two 3T whole-body scanners. 14 carriers of a 16p11.2 deletion and 17 duplication carriers, together with 59 controls (21 familial and 38 unrelated controls) were examined on a Magnetom TIM Trio (Siemens Healthcare, Erlangen, Germany), using a 12-channel RF receive head coil and RF body transmit coil. The remaining 16p11.2 (13 deletions, 6 duplications), 1q11.2 (9 deletions, 7 duplications) carriers and controls (n=38) in the european cohort, were scanned on a Magnetom Prisma Syngo (Siemens Healthcare, Erlangen, Germany) using a 64-channel RF receive head coil and RF body transmit coil. T1-weighted (T1w) anatomical images acquired with the TIM Trio scanner used a Multi-Echo Magnetization Prepared RApid Gradient Echo sequence (ME-MPRAGE: 176 slices; 256×256 matrix; echo time (TE): TE1 = 1.64 ms, TE2 = 3.5 ms, TE3 = 5.36 ms, TE4 = 7.22 ms; repetition time (TR): 2530 ms; flip angle 7°). On the Prisma Syngo scanner, T1w images were acquired using a single-echo MPRAGE sequence (176 slices; 256×256 matrix; TE = 2.39 ms; TR = 2000 ms; flip angle 9°).

Simons VIP study

Data were acquired using multi and single-echo sequences. 176 participants (38 del/ 34 dup 16p11.2 carriers, 2 dup 1q21.1 carriers and 102 familial controls) underwent the research MRI protocol at two imaging core sites on matched 3T Magnetom TIM Trio MRI scanners (Siemens Healthcare, Erlangen, Germany), using the vendor-supplied 32-channel phased-array radio-frequency head coils. 68 participants were scanned at University of California sites (UC) and 108 at the Children Hospital of Philadelphia (CHOP). Structural MRI data included multi-echo T1w ME-MPRAGE using the following parameters: 176 slices, 256×256 matrix, TR = 2530 ms, TI = 1200 ms, TE = 1.64 ms, and flip angle 7°. Clinical MRI images (single-echo) obtained at the phenotyping core sites were also analyzed. The remaining 79 subjects (19 del/ 13 dup 16p11.2 carriers, 12 del/8 dup 1q21.1 carriers and 27 familial controls) were scanned at University of Washington Medical Center, Baylor University Medical Center and Boston Children's Hospital on two matched 3T Philips Achieva (Philips Healthcare, United States of America) and one unmatched Magnetom TIM Trio scanner (Siemens Healthcare, Erlangen, Germany), respectively. T1w images were acquired using a single-echo MPRAGE sequence and the following parameters: 160 slices; 256×256 matrix; TE = 2.98 ms; TR = 2300 ms; flip angle 9°. All multi-echo images were averaged following a Root-Mean Square (RMS) averaging method.

Brain Canada

MRI scans for the Brain Canada cohort have been performed at the Montreal Neurological Institute with the same 3T scanner: Magnetom Prisma Syngo (Siemens Healthcare, Erlangen, Germany). Data included 16p11.2 (3 deletions, 3 duplications), 1q11.2 (5 deletions, 1 duplication), 22q11.2 (1 duplication) carriers and controls (n=26) T1w images were acquired using using MPRAGE sequences, scanning protocol description is detailed on this website: http://www.bic.mni.mcgill.ca/users/jlewis/BrainCanada/MCIN/.

UCLA

Imaging data of 22q11.2 CNV carriers and typically developing (TD) controls were acquired at the University of California, Los Angeles (UCLA). Patients were ascertained from the UCLA or Children's Hospital, Los Angeles Pediatric Genetics, Allergy/Immunology and/or Craniofacial Clinics. We excluded xx individuals from the analysis due to insufficient quality of the imaging data (cf. Supplementary Methods, quality control). The final 22q11.2 sample includes 144 individuals (71 deletions, 19 duplications and 54 controls). Demographically comparable TD comparison subjects were recruited from the same communities as patients via web-based advertisements and by posting flyers and brochures at local schools, pediatric clinics, and other community sites. Exclusion criteria for all study participants included significant neurological or medical conditions (unrelated to 22q11.2 mutation) that might affect brain structure, history of head injury with loss of consciousness, insufficient fluency in English, and/or substance or alcohol abuse or dependence within the past 6 months. The UCLA Institutional Review Board approved all study procedures and informed consent documents. Scanning was conducted on an identical 3 tesla Siemens Trio MRI scanner with a 12-channel head coil at the University of California at Los Angeles Brain Mapping Center or at the Center for Cognitive Neuroscience.

Cardiff

Imaging acquisition in Cardiff was performed on a 3 T General Electric HDx MRI system (GE Medical Systems, Milwaukee, WI) using an eight-channel receive-only head RF coil. T1-weighted structural images were acquired with a 3D fast spoiled gradient echo (FSPGR) sequence (TR = 7.8 ms, TE = 3.0 ms, voxel size = 1 mm^3 isomorphic). Data included 1 16p11.2 deletion, 1q11.2 (3 deletions, 1 duplication), 22q11.2 (3 deletions, 2 duplications) carriers and 15 controls.

MRI quality control

All MRI T1w nifti images were visually inspected by the same rater (CM) for head coverage, ghosting and susceptibility artifacts. Images were also screened after segmentation to ensure good tissue classification accuracy. From the clinically ascertained dataset 55 subjects were excluded for insufficient image quality or artifacts while from the non-clinically ascertained dataset 52 subjects were excluded following the same criteria. Quality assurance protocol for Freesurfer based cortical reconstructions led to exclusion of an additional 34 scans.

List of abbreviations

CNV: Copy Number Variant, ASD: Autism Spectrum Disorders, SCZ: Schizophrenia, VBM: Voxel Based Morphometry, SBM: Surface Based Morphometry, TIV: Total Intracranial Volume, GM: Grey Matter, WM: White Matter, ICV: Intracranial Volume, CT: Cortical Thickness, SA: Surface Area, IQ: Intelligence Quotient, CCA: Canonical Correlation Analysis, pLI: Probability of being loss-of-function intolerant.

eMethod 1: MRI data processing, Voxel-Based Morphometry

We used the probabilistic tissue classification within SPM12 "unified segmentation" framework [26] and enhanced tissue priors for optimal delineation of subcortical structures [27]. The obtained grey and white matter maps were screened for tissue misclassification by the same researcher (CM). Individuals' gray matter (GM) maps were subsequently spatially registered to the standard Montreal Neurological Institute (MNI) space using DARTELs diffeomorphic registration [28] followed by voxel-based scaling using the Jacobian determinants of the deformation field (i.e., "modulation"). Finally, GM maps were smoothed

with a Gaussian of 8mm full-width-at-half-maximum. Parcellation into regions of interest (ROIs) was performed using maximum probability tissue labels (http://www.neuromorphometrics.com/) build using data from the OASIS project (http://www.oasis-brains.org). ROIs' volumes obtained for each subject were used as one of the inputs for canonical correlation analysis, with the exception of white matter ROIs that were excluded.

eMethod 2: MRI data processing, Surface-Based Morphometry

ENIGMA quality control procedures (http://enigma.ini.usc.edu/protocols/imaging-protocols/) led to the exclusion of additional 34 scans. Applying FreeSurfer's recon-all pipeline, estimates of local cortical thickness (CT) and surface area (SA) were calculated at each vertex. Statistical analyses were conducted on each vertex (Freesurfer fsaverage, 327,684 vertices), after spatially smoothing with a Gaussian kernel of 10-mm full width at half maximum (FWHM). In addition, FreeSurfer provided estimates of global brain measures of mean cortical thickness, total surface area per hemisphere, and regional measures based on the Desikan Freesurfer atlas [30].

eMethod 3: Multi-view pattern-learning analysis

Canonical correlation analysis (CCA) allows a single integrated multivariate analysis to simultaneously co-analyze brain morphometry measures along with the Genomic loci information (CNV status). This aims to identify symmetric linear relations between the two sets of variables. In our study, the first variable set (X) represents the CNV status of a subject, based on encoding with -1 (deletion) 0 (normal diploid) or +1 (duplication). All regional volume measures were normalized by de-meaning to 0 and re-scaling to 1. That is, the set of CNV carrier status was jointly encoded, capturing genomic loci. The second variable set (Y) was encoded as a matrix of 130 regional grey matter volumes (68 Desikan ROIs for SA, and CT) adjusted for total grey matter volume (Total SA, and Mean CT for SA, and CT).

The brain volume measures in variable set Y were fed into CCA after a confound-removal procedure including age, age^2, sex, site, and total grey matter analogous to previous studies [31–33].

Our CCA strategy involved finding pairs of canonical vectors u and v that maximize the correlation in the embedding space (canonical variates) between a linear combination of the set of CNV indicators (X) and a linear combination of regional volumes (Y). In other words, canonical vectors project high dimensional variable sets onto a new low-rank space defined by the linear combination of original variables, called canonical variates. The Canonical Correlation, calculated as Pearson's correlation (r) between X and Y canonical variates, can be seen as a metric of joint information reduction and serves as a performance measure for CCA. In our study, CCA identifies modes of coherent co-variation that jointly characterize how CNVs and patterns of regional volumes systematically co-occur across subjects. We refer to these modes of co-variation as 'CCA dimensions' or 'gene-morphology dimensions'.

The statistical significance of the derived dominant modes of gene-morphology co-variation was determined by null hypothesis testing based on a non-parametric permutation procedure [31]. Relying on minimal modeling assumptions [34], an empirical null distribution representing the absence of correlation between CNVs and brain morphometry. 1,000 gene-volume correlations were computed after permuting the original data such that the CNV status and set of region volume expressions were unrelated across individuals. In 1,000 permutation iterations, the CNV labels were held constant, while the regional volumes were subject to participant-wise random shuffling. The CCA analysis was rerun for each permutation iteration (the maximum possible correlation coefficient). An original CCA dimension was declared statistically significant if the associated canonical correlation values exceeded the 99% percentile of the null distribution (i.e., $p<0.01$).

eMethod 4: Voxel-based measures and statistical analyses

GM maps were entered as dependent variables, group - as independent variable (variance between groups was set as unequal) and age, age^2, sex, scanning site, total grey matter volume - as fixed effects. After

model estimation, post hoc contrasts were calculated to compare each CNV group to the corresponding control group. VBM results on grey matter are significant at $p<0.05$, FWE corrected [13–15]. We tested for significant effects in a conjunction analysis across the pre-defined contrasts.

eMethod 5: Spin permutation testing

To perform the spin permutation test, we applied 10,000 random surface-based rotations of XYZ to a given map, generating random maps while preserving the relative spatial organization of the vertices. We then generate a null distribution of dice indices or correlation values for deletion and duplication convergence patterns or deletion-duplication anti-correlation respectively. An empirical p-value ($p\text{-value}_{SPIN}$) was then obtained as the proportion of 10,000 null dice-indices or correlations that had a higher value than the observed value. $P\text{-value}_{SPIN} < 0.05$ was used as a statistical significance threshold [37,38].

eMethod 6: Label shuffling

We performed permutation for control and CNV labels (7 groups, clinically ascertained) 10,000 times, and calculated the same overlap using the 15th and 85th percentile of Cohen's d values (the top 15% of positive and negative effect sizes) between the three random groups. For 15q11.2 CNVs (non-clinically ascertained), we shuffled control and CNV labels 10,000 times. We then calculated the same overlap using the 15th and 85th percentile of Cohen's d values (the top 15% of positive and negative effect sizes) with 3-deletion convergence pattern (cf. above). To generate empirical null distributions to obtain p-values ($p\text{-value}_{SHUFFLE}$) for significance testing, we calculated dice index distribution w.r.t the convergence pattern. Similarly, for a new map, we calculated the dice index with respect to the convergence pattern and 10,000 random patterns generated above. An empirical p-value ($p\text{-value}_{SHUFFLE}$) was then obtained based on the proportion of 10,000 random map based dice-indices that had a higher value than the observed value. $p\text{-value}_{SHUFFLE} < 0.05$ was used as a statistical significance threshold [37,38]

CLINICAL ASCERTAINMENT										
CNV loci	Copy number	Cohort	Age mean(SD)	Age mean(SD)	Male/Female	Male/Female	TIV mean(SD)	TIV mean(SD)	FSIQ mean(SD)	FSIQ mean(SD)
1q21.1	Deletions *N=29*	EU *N=9*	29.43 (18.40)	18.91 (12.91)	11/18	1/8	1.22 (0.14)	1.15 (0.09)	90.85 (21.75) *N=26*	81.67 (21.57) *N=9*
		VIP *N=12*		35.11 (20.66)		6/6		1.27 (0.15)		99.33 (23.96) *N=12*
		BC *N=5*		28.25 (18.46)		1/4		1.17 (0.17)		87 (4.76) *N=5*
		Cardiff *N=3*		40.18 (13.15)		3/0		1.36 (0.02)		(-)
	Duplications *N=19*	EU *N=7*	34.29 (17.19)	37.32 (19.58)	10/9	5/2	1.57 (0.11)	1.58 (0.07)	95.56 (23.19) *N=18*	96.57 (11.59) *N=7*
		VIP *N=10*		34.25 (15.84)		5/5		1.54 (0.13)		93.80 (30.17) *N=10*
		BC *N=1*		8.34 (-)		0/1		1.57 (-)		106 (-) *N=1*
		Cardiff *N=1*		39.45 (-)		0/1		1.76 (-)		(-)
16p11.2	Deletions *N=83*	EU *N=26*	17.14 (11.97)	21.23 (13.51)	47/36	15/11	1.54 (0.17)	1.44 (0.14)	82.17 (14.99) *N=64*	74.38 (14.61) *N=13*
		VIP *N=53*		13.82 (9.47)		30/23		1.58 (0.17)		83.98 (14.36) *N=48*
		BC *N=3*		31.64 (10.26)		1/2		1.46 (0.09)		87 (21) *N=3*
		Cardiff *N=1*		43.04 (-)		1/0		2.01 (-)		(-)
	Duplications *N=73*	EU *N=23*	31.01(14.91)	32.55 (13.20)	41/32	13/10	1.33 (0.17)	1.36 (0.16)	85 (19.70) *N=63*	72.71 (16.30) *N=17*
		VIP *N=47*		30.52 (15.30)		25/22		1.30 (0.15)		90.44 (18.49) *N=43*
		BC *N=3*		26.89 (25.29)		3/0		1.49 (0.42)		86.67 (23.50) *N=3*
22q11.2	Deletions *N=74*	UCLA *N=71*	16.35 (8.56)	15.66 (7.24)	35/39	34/37	1.30 (0.15)	1.30 (0.15)	77.42 (13.51) *N=48*	77.41 (13.51) *N=50*
		Cardiff *N=3*		32.56 (20.60)		1/2		1.37 (0.11)		(-)
	Duplications *N=22*	UCLA *N=19*	19.66 (14.24)	17.32 (12.51)	15/7	13/6	1.47 (0.16)	1.45 (0.17)	97.83 (20.34) *N=12*	99.18 (20.76) *N=11*
		BC *N=1*		13.67 (-)		1/0		1.50 (-)		83 (-) *N=1*
		Cardiff *N=2*		44.94 (4.77)		1/1		1.55 (0.16)		(-)
Controls *N=331*		EU *N=97*	25.91 (14.57)	30.33 (12.95)	189/142	62/35	1.46 (0.15)	1.49 (0.14)	106.73 (15.03) *N=224*	102.15 (12.98) *N=59*
		VIP *N=129*		24.03 (14.56)		71/58		1.44 (0.14)		108.88 (11.82) *N=90*
		UCLA *N=54*		13.37 (4.96)		30/24		1.39 (0.13)		112.43 (20.95) *N=44*
		BC *N=36*		33.56 (14.90)		19/17		1.52 (0.17)		101.11 (13.18) *N=31*
		Cardiff *N=15*		40.18 (11.12)		7/8		1.54 (0.15)		(-)

NON-CLINICAL ASCERTAINMENT						
CNV loci	Copy number	Cohort	Age mean(SD)	Male/Female	TIV mean(SD)	UKB FI mean(SD)
1q21.1	Deletions *N=10*	UKBB	59.11 (6.71)	6/4	1.35 (0.12)	-0.8 (0.5) *N=9*
	Duplications *N=9*		60.56 (7)	2/7	1.55 (0.14)	0.2 (1.3) *N=9*
15q11.2	Deletions *N=72*		63.38 (7.60)	31/41	1.54 (0.15)	-0.3 (0.9) N=63
	Duplications *N=76*		62.92 (7.31)	36/40	1.49 (0.15)	0 (1.1) *N=71*
16p11.2	Deletions *N=4*		65.6 (3.2)	3/1	1.56 (0.13)	0.8 (0.5) *N=2*
	Duplications *N=4*		69.3 (2.1)	1/3	1.29 (0.11)	-1.6 (0.2) *N=4*
22q11.2	Deletions *N=1*		69.8 (-)	31/41	1.44 (-)	-
	Duplications *N=8*		62 (9.5)	4/4	1.55 (0.17)	-0.2 (1.1) *N=8*
Controls *N=965*			62.13 (7.40)	358/607	1.51 (0.14)	0 (1) *N=866*

eTable 1 : Demographics

Legend: CNV: Copy Number Variant, SD: Standard deviation, TIV: total intracranial volume, FSIQ: Full-scale IQ, UKB FI: UK Biobank fluid intelligence, ASD: Autism Spectrum Disorders, SCZ: schizophrenia (including * ICD10 code F25.9 Schizoaffective disorder, unspecified). CNV carriers and controls from the clinically ascertained group come from 5 different cohorts, while non-clinically ascertained participants were identified in the UK Biobank. UK Biobank fluid intelligence scores (UKB

field:20016) were adjusted for age, age^2, sex, site, and then z-scored. 16p11.2 and 22q11.2 from the UKBB were not included in the VBM and SBM due to small sample size.

	Median Cohen's d 5th percentile	Median Cohen's d 95th percentile	% of voxels surviving FWE	% of voxels with negative effects surviving FWE	% of voxels with positive effects surviving FWE
1q21.1 deletion	-0.29	0.30	1.49%	0.64%	0.84%
1q21.1 duplication	-0.23	0.22	0.04%	0.01%	0.03%
16p11.2 deletion	-0.48	0.65	17.13%	8.03%	9.09%
16p11.2 duplication	-0.37	0.25	2.84%	2.66%	0.17%
22q11.2 deletion	-0.45	0.59	14.81%	7.28%	7.52%
22q11.2 duplication	-0.23	0.27	0.32%	0.06%	0.26%
1q21.1 deletion UKBB	-0.14	0.17	0.31%	-	0.31%
1q21.1 duplication UKBB	-0.14	0.15	0.04%	-	0.04%
15q11.2 deletion UKBB	-0.13	0.14	0.02%	0.02%	-
15q11.2 duplication UKBB	-0.12	0.14	0.002%	-	0.002%

eTable 2: CNV effect sizes on local grey matter volume changes.

Legend: First and second column report medians of 5th and 95th percentiles of Cohen's d distributions. Columns three to five report voxels surviving FWE error correction.

	Median Cohen's d 5th percentile	Median Cohen's d 95th percentile	% of vertices surviving FDR (q<0.05)	% of vertices with negative effects surviving FDR (q<0.05)	% of vertices with positive effects surviving FDR (q<0.05)
1q21.1 deletion	-0.21	0.21	0.31%	-	0.31%
1q21.1 duplication	-0.18	0.20	0.06%	-	0.06%
16p11.2 deletion	-0.51	0.63	42.45%	19.97%	22.48%
16p11.2 duplication	-0.35	0.30	13.91%	8.81%	5.10%
22q11.2 deletion	-0.44	0.49	34.07%	14.60%	19.47%
22q11.2 duplication	-0.18	0.21	1.31%	0.31%	1.00%
1q21.1 deletion UKBB	-0.11	0.11	-	-	-
1q21.1 duplication UKBB	-0.12	0.15	0.10%	0.03%	0.07%
15q11.2 deletion UKBB	-0.12	0.13	0.07%	-	0.07%
15q11.2 duplication UKBB	-0.13	0.14	-	-	-

eTable 3: CNV effect sizes on local Surface Area changes.

Legend: First and second column report medians of 5th and 95th percentiles of Cohen's d distributions.

Columns three to five report vertices surviving FDR correction (q<0.05).

	Median Cohen's d 5th percentile	Median Cohen's d 95th percentile	% of vertices surviving FDR (q<0.05)	% of vertices with negative effects surviving FDR (q<0.05)	% of vertices with positive effects surviving FDR (q<0.05)
1q21.1 deletion	-0.21	0.24	2.44%	0.55	1.89%
1q21.1 duplication	-0.20	0.18	-	-	-
16p11.2 deletion	-0.31	0.35	18.31%	8.67%	9.64%
16p11.2 duplication	-0.27	0.26	6.88%	4.02%	2.86%
22q11.2 deletion	-0.44	0.39	27.96%	18.52%	9.44%
22q11.2 duplication	-0.22	0.20	0.71%	0.46%	0.25%
1q21.1 deletion UKBB	-0.12	0.14	-	-	-
1q21.1 duplication UKBB	-0.23	0.08	19.23%	19.23%	-
15q11.2 deletion UKBB	-0.12	0.14	-	-	-
15q11.2 duplication UKBB	-0.11	0.12	-	-	-

eTable 4: CNV effect sizes on local Cortical Thickness changes.

Legend: First and second column report medians of 5th and 95th percentiles of Cohen's d distributions. Columns three to five report vertices surviving FDR correction (q<0.05).

	ROI	|CC1|	ROI	|CC2|
1.	Left_transverse_temporal_gyrus	0.54424372	Right_Accumbens_Area	0.716341907
2.	Left_planum_temporale	0.516375486	Left_Accumbens_Area	0.693450348
3.	Left_parietal_operculum	0.478605816	Left_subcallosal_area	0.598630484
4.	Left_calcarine_cortex	0.434979442	Left_cuneus	0.587180378
5.	Right_supplementary_motor_cortex	0.423161744	Left_precuneus	0.542742079
6.	Right_calcarine_cortex	0.417872614	Brain_Stem	0.538584491
7.	Left_posterior_insula	0.41658809	Right_superior_frontal_gyrus	0.530594854
8.	Left_middle_cingulate_gyrus	0.404137535	Cerebellar_Vermal_Lobules_VIII-X	0.530148089
9.	Left_middle_temporal_gyrus	0.380330333	Left_anterior_insula	0.527867312
10.	Right_anterior_insula	0.378170585	Right_lingual_gyrus	0.526385942
11.	Right_posterior_orbital_gyrus	0.375392577	Left_lingual_gyrus	0.52497161
12.	Left_anterior_insula	0.37348146	Right_cuneus	0.513604455
13.	Right_occipital_pole	0.367616101	Right_Caudate	0.502454679
14.	Left_supplementary_motor_cortex	0.35555794	Right_anterior_insula	0.49874064
15.	Right_precentral_gyrus	0.354152555	Left_calcarine_cortex	0.486781547
16.	Right_posterior_insula	0.352835632	Left_superior_frontal_gyrus	0.481515906
17.	Right_middle_temporal_gyrus	0.351133642	Left_Cerebellum_Exterior	0.477760835
18.	Right_middle_cingulate_gyrus	0.343736614	Left_gyrus_rectus	0.468197071
19.	Right_middle_frontal_gyrus	0.341059273	Right_subcallosal_area	0.465928639
20.	Left_Thalamus_Proper	0.340754975	Right_calcarine_cortex	0.463409682

eTable 5: Canonical Correlation Analysis ROIs loadings.

Legend: Top 20 loadings of Neuromorphometric Regions of Interests (ROIs) on the 2 main CCA dimensions (r=0.84, 0.79; statistically significant at p-value<0.01). Loadings are in absolute values and listed in decreasing order.

	ROI	|CC1|		ROI	|CC2|
1.	L_superiortemporal	0.6587446385		R_supramarginal	0.4556194543
2.	R_superiortemporal	0.4716305815		R_postcentral	0.4078724885
3.	R_pericalcarine	0.3752495588		L_caudalanteriorcingulate	0.3529766412
4.	L_bankssts	0.3625881379		L_postcentral	0.3515379435
5.	L_transversetemporal	0.3385850519		R_pericalcarine	0.3243996464
6.	L_insula	0.3145652172		L_inferiortemporal	0.3037588837
7.	R_caudalanteriorcingulate	0.3088200827		R_inferiortemporal	0.2836174352
8.	L_parahippocampal	0.3074088432		L_parstriangularis	0.2467471024
9.	L_caudalanteriorcingulate	0.2822321503		R_superiortemporal	0.2382066534
10.	L_lingual	0.2806560547		L_fusiform	0.2357128834
11.	L_pericalcarine	0.2775258853		L_lingual	0.2303667725
12.	L_inferiorparietal	0.249919579		R_fusiform	0.2224770313
13.	R_insula	0.243533976		L_pericalcarine	0.2217702203
14.	L_inferiortemporal	0.2406929256		R_lateraloccipital	0.2163886563
15.	R_lingual	0.2355838232		L_cuneus	0.2143733739
16.	R_posteriorcingulate	0.2275119787		R_superiorparietal	0.2064224327
17.	L_fusiform	0.2234845007		L_supramarginal	0.2042270199
18.	R_bankssts	0.2160471626		L_lateralorbitofrontal	0.200380036
19.	L_superiorparietal	0.213339904		L_lateraloccipital	0.1888223609
20.	R_cuneus	0.2122297907		R_rostralanteriorcingulate	0.1811606572

eTable 6: Canonical Correlation Analysis ROIs loadings (CT).

Legend: Top 20 loadings of Desikan Regions of Interests (ROIs) on the 2 main CCA dimensions (r=0.69, 0.65; statistically significant at p-value<0.01). Loadings are in absolute values and listed in decreasing order.

	ROI	|CC1|		ROI	|CC2|
1.	L_bankssts	0.6521173442		L_cuneus	0.4721872379
2.	L_lateraloccipital	0.6217516421		R_precentral	0.4287453486
3.	L_insula	0.5772778171		L_caudalmiddlefrontal	0.3853658259
4.	R_bankssts	0.5730431727		L_lingual	0.3836281323
5.	R_lateraloccipital	0.5575884583		L_precentral	0.3658962124
6.	R_insula	0.5274745577		R_lingual	0.3579919796
7.	R_lingual	0.4881908917		R_superiorfrontal	0.3560307613
8.	L_pericalcarine	0.4619077081		L_lateralorbitofrontal	0.3541644729
9.	L_lateralorbitofrontal	0.443217953		L_insula	0.3306590802
10.	L_entorhinal	0.4227964373		R_insula	0.3119737927
11.	R_pericalcarine	0.4101667004		L_precuneus	0.3104848234
12.	L_lingual	0.4071596452		R_cuneus	0.3006340465
13.	R_parsorbitalis	0.4015238848		R_precuneus	0.2940527986
14.	L_postcentral	0.3973332167		L_superiorparietal	0.2856777808
15.	L_caudalmiddlefrontal	0.3914227421		R_lateralorbitofrontal	0.2854749482
16.	L_middletemporal	0.3882833195		R_superiorparietal	0.2735339712
17.	R_middletemporal	0.3879412723		L_superiorfrontal	0.271298681
18.	R_caudalmiddlefrontal	0.3821714147		L_pericalcarine	0.2670122335
19.	L_inferiortemporal	0.379691104		R_parsopercularis	0.2515318479
20.	R_superiorfrontal	0.3789751734		L_postcentral	0.2398170347

eTable 7: Canonical Correlation Analysis ROIs loadings (SA).

Legend: Top 20 loadings of Desikan Regions of Interests (ROIs) on the 2 main CCA dimensions (r=0.79, 0.67; statistically significant at p-value<0.01). Loadings are in absolute values and listed in decreasing order.

	1q21.1	16p11.2	22q11.2	ukb1q21.1	ukb15q11.2
1q21.1	-0.187	-0.058	0.258*	0.213*	0.150
16p11.2	0.141	-0.626*	-0.141	0.035	-0.025
22q11.2	0.035	0.208	-0.232*	-0.006	-0.061
ukb1q21.1	0.535*	0.064	0.058	-0.384*	0.083
ukb15q11.2	-0.138	0.020	0.173	-0.175	-0.184

eTable 8: Brain-wide Cohen's d map Correlations for VBM

Legend: Pearson correlation between Cohen's d maps (brain wide) for Deletion-Duplication (Diagonal, purple cells), Deletion-Deletion (Lower triangle, red cells), and Duplication-Duplication (Upper triangle, blue cells) for clinical and non-clinical CNVs. ukb15q11.2 and ukb1q21.1 correspond to UKBB CNV carriers. * Bonferoni correction, p-value$_{SPIN}$ <0.002 (=0.05/25).

	1q21.1	16p11.2	22q11.2	ukb1q21.1	ukb15q11.2
1q21.1	-0.147	0.232*	-0.030	0.318*	0.021
16p11.2	0.136	-0.551*	-0.006	0.083	0.025
22q11.2	0.111	0.133	-0.139	0.035	0.050
ukb1q21.1	0.332*	0.118	-0.143	-0.275*	0.041
ukb15q11.2	0.058	0.054	0.178	-0.035	-0.231*

eTable 9: Cortex-wide Cohen's d map Correlations for SA

Legend: Pearson correlation between Cohen's d maps (coretx wide) for Deletion-Duplication (Diagonal, purple cells), Deletion-Deletion (Lower triangle, red cells), and Duplication-Duplication (Upper triangle, blue cells) for clinical and non-clinical CNVs. ukb15q11.2 and ukb1q21.1 correspond to UKBB CNV carriers. * Bonferoni correction, p-value$_{SPIN}$ <0.002 (=0.05/25).

	1q21.1	16p11.2	22q11.2	ukb1q21.1	ukb15q11.2
1q21.1	-0.074	0.083	0.165	0.059	0.041
16p11.2	0.132	-0.169	-0.094	-0.068	0.066
22q11.2	-0.037	0.032	0.012	0.198	-0.044
ukb1q21.1	0.381*	0.123	-0.130	-0.103	-0.009
ukb15q11.2	0.032	0.074	-0.016	0.115	-0.092

eTable 10: Cortex-wide Cohen's d map Correlations for CT

Legend: Pearson correlation between Cohen's d maps (coretx wide) for Deletion-Duplication (Diagonal, purple cells), Deletion-Deletion (Lower triangle, red cells), and Duplication-Duplication (Upper triangle, blue cells) for clinical and non-clinical CNVs. ukb15q11.2 and ukb1q21.1 correspond to UKBB CNV carriers. * Bonferoni correction, p-value$_{SPIN}$ <0.002 (=0.05/25).

	Ratio del/dup (GM)	F test del/dup (GM)	Degrees of freedom df1-df2 (GM)	p-value *F* test (GM)	Ratio del/dup (SA)	F test del/dup (SA)	Degrees of freedom df1-df2 (SA)	p-value *F* test (SA)
1q21.1	1.297	1.682	416407-416408	0	1.087	1.174	327683-327683	0
16p11.2	1.846	3.485	416408-416408	0	1.772	3.141	327683-327683	0
22q11.2	2.019	4.0748	416408-416407	0	2.267	5.139	327683-327683	0
ukb 1q21.1	1.013	1.025	385045-385046	0	0.795	0.631	327683-327683	0
ubk 15q11.2	1.071	1.148	385045-385045	0	0.944	0.892	327683-327683	0

eTable 11: Within loci comparison of Cohen's d variances between deletions and duplications.

Legend: Standard deviation ratio and two-sample *F* test for equal variances on Cohen's D distributions of GM volume and SA. Second and sixth columns report standard deviations ratios between deletion and duplication Cohen's d distributions. Column 3-5 and 7-9 report two-sample F test statistics for GM volume and SA for each loci.

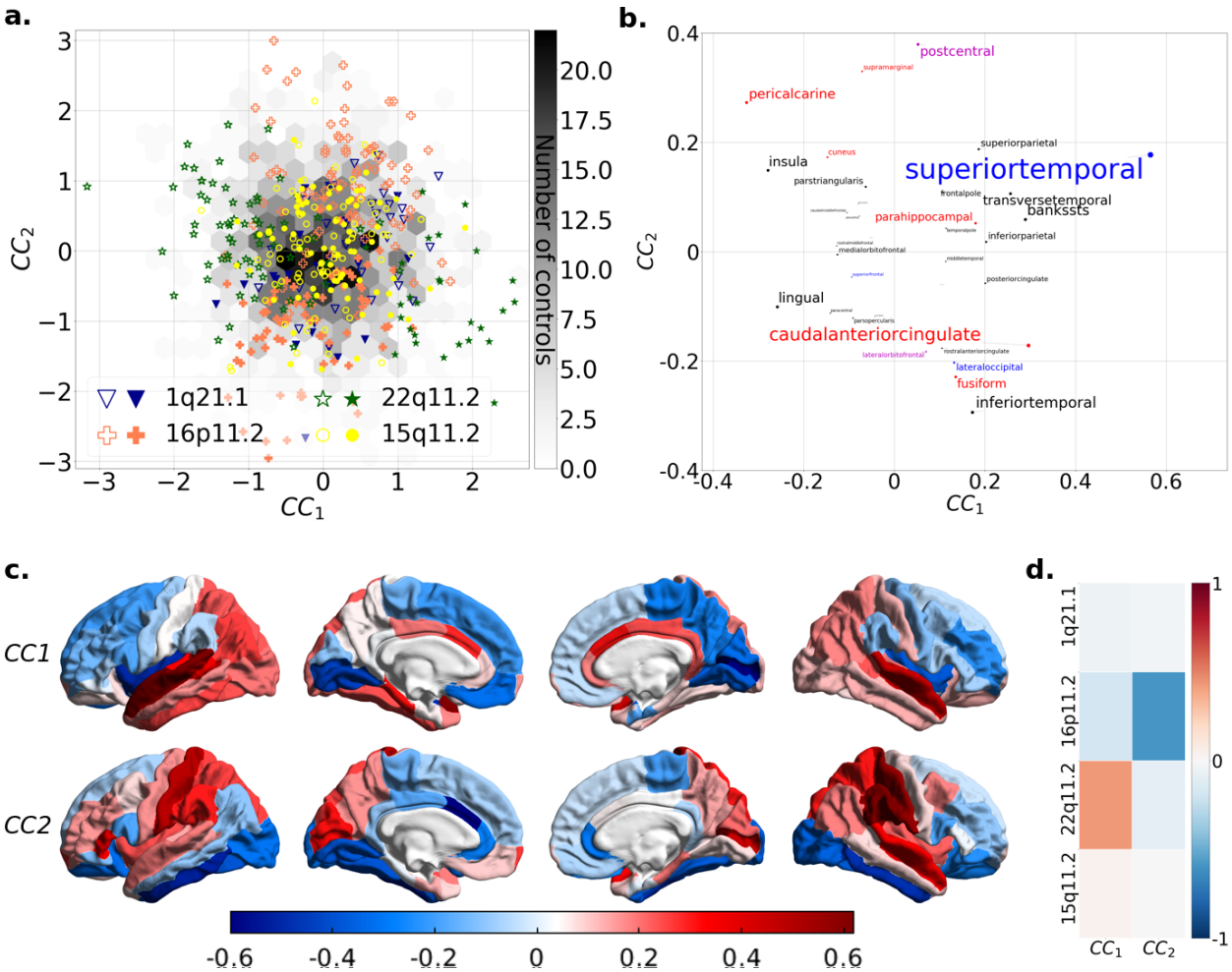

eFigure 1: CCA analysis across 4 CNVs Cortical Thickness.

Legend: (a) Scatterplot showing the position of each of the 468 carriers of 8 different CNVs along 2 Canonical Correlation (CC) dimensions established using 68 Freesurfer regions of CNV carriers. Cortical Thickness (CT) was calculated using Freesurfer recon-all and was adjusted for mean CT, age, age^2, sex, and site. The empty and full symbols represent deletions and duplication respectively. The grey hexagonal bin plot represents the frequency of controls (n=1252). Controls were not used to compute the CCA and were projected post hoc on the 2 dimensions using CCA prediction. X and Y axis values: z-scores of regional volumes. (b) Loading of Freesurfer Regions of Interests (ROIs) on the 2 CC dimensions. X-axis and Y-axis values: normalized values from (-1 to +1) of dimensions 1 and 2 respectively. The font size is

correlated to the region's contribution to CC dimensions. ROI names are color-coded as being part of the deletion (red), duplication (blue) and both deletion and duplication (magenta) convergence patterns. (c) CCA dimensions 1 and 2 projected on the brain. Brain regions most strongly associated with CCA dimensions 1 and 2. The darker the red or blue color, the stronger the positive or negative association with the CCA dimensions. (d) Loading of the first and second CCA dimensions on 4 CNV genomic loci. Values are CCA loading magnitudes and represent the contribution of a CNV locus to the canonical dimension. CCA was calculated using 449 CNV carriers without controls and identified 3 dimensions (r=0.69, 0.65, 0.58; statistically significant at p-value<0.01). Top 20 ROI loadings (absolute values) for CC1 and CC2 are listed in eTable 7.

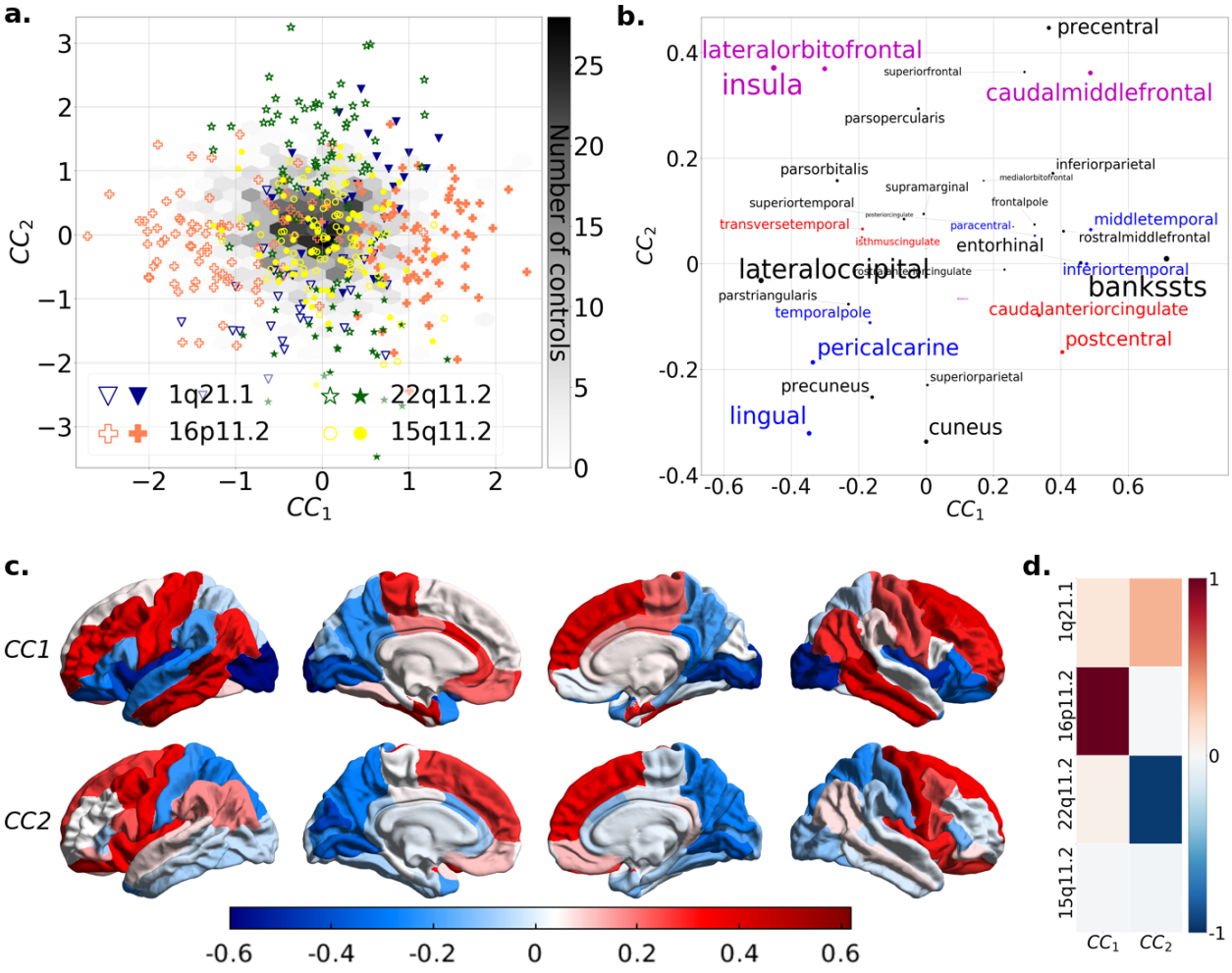

eFigure 2: CCA analysis across 4 CNVs Surface Area.

Legend: (a) Scatterplot showing the position of each of the 468 carriers of 8 different CNVs along 2 Canonical Correlation (CC) dimensions established using 68 Freesurfer regions of CNV carriers. Surface Area (SA) was calculated using Freesurfer recon-all and were adjusted for mean total SA, age, age^2, sex and site. The empty and full symbols represent deletions and duplication respectively. The grey hexagonal bin plot represents the frequency of controls (n=1252). Controls were not used to compute the CCA and were projected post hoc on the 2 dimensions using CCA prediction. X and Y axis values: z-scores of regional volumes. (b) Loading of Freesurfer Regions of Interests (ROIs) on the 2 CC dimensions. X axis and Y axis values: normalized values from (-1 to +1) of dimensions 1 and 2 respectively. The font size is correlated to the region's contribution to CC dimensions. ROI names are color coded as being part of the deletion (red), duplication (blue) and both deletion and duplication (magenta) convergence patterns. (c) CCA dimensions 1 and 2 projected on the brain. Brain regions most strongly associated with CCA dimensions 1 and 2. The darker the red or blue color, the stronger the positive or negative association with the CCA dimensions. (d) Loading of the first and second CCA dimensions on 4 CNV genomic loci. Values are CCA loading magnitudes and represent the contribution of a CNV loci to the canonical dimension. CCA was calculated using 449 CNV carriers without controls and identified 3 dimensions (r=0.79, 0.67, 0.56; statistically significant at p-value<0.01). Top 20 ROI loadings (absolute values) for CC1 and CC2 are listed in eTable 8.

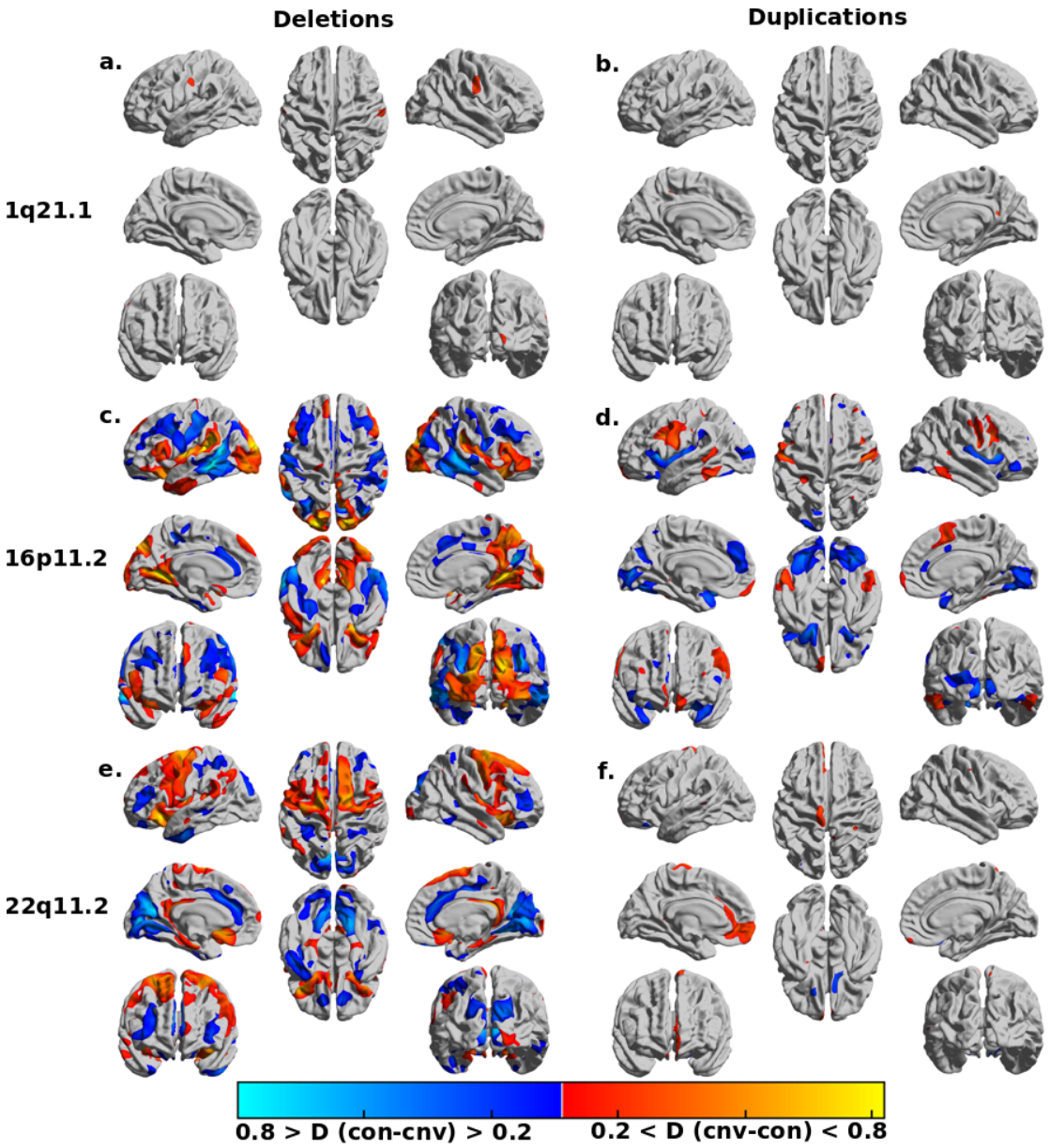

eFigure 3: FDR corrected Cohen's d maps of Surface Area.

Legend: Vertex-wise brain differences in deletion and duplication carriers at the 1q21.1, 16p11.2 and 22q11.2. loci. 15q11.2 was not displayed because few vertices survived FDR correction. The left column shows regional brain differences for deletion carriers (a, c, e) while right columns show regional brain differences for duplication carriers (b, d, f). Cohen's d effect sizes were estimated in SurfStat using vertex-wise SA estimate maps obtained from Freesurfer. Linear model was adjusted for sex, linear and

quadratic expansion of age and total surface area. The results are significant at the FDR threshold q < 0.05, and shown within a range of 0.2 and 0.8 for comparison across CNVs.

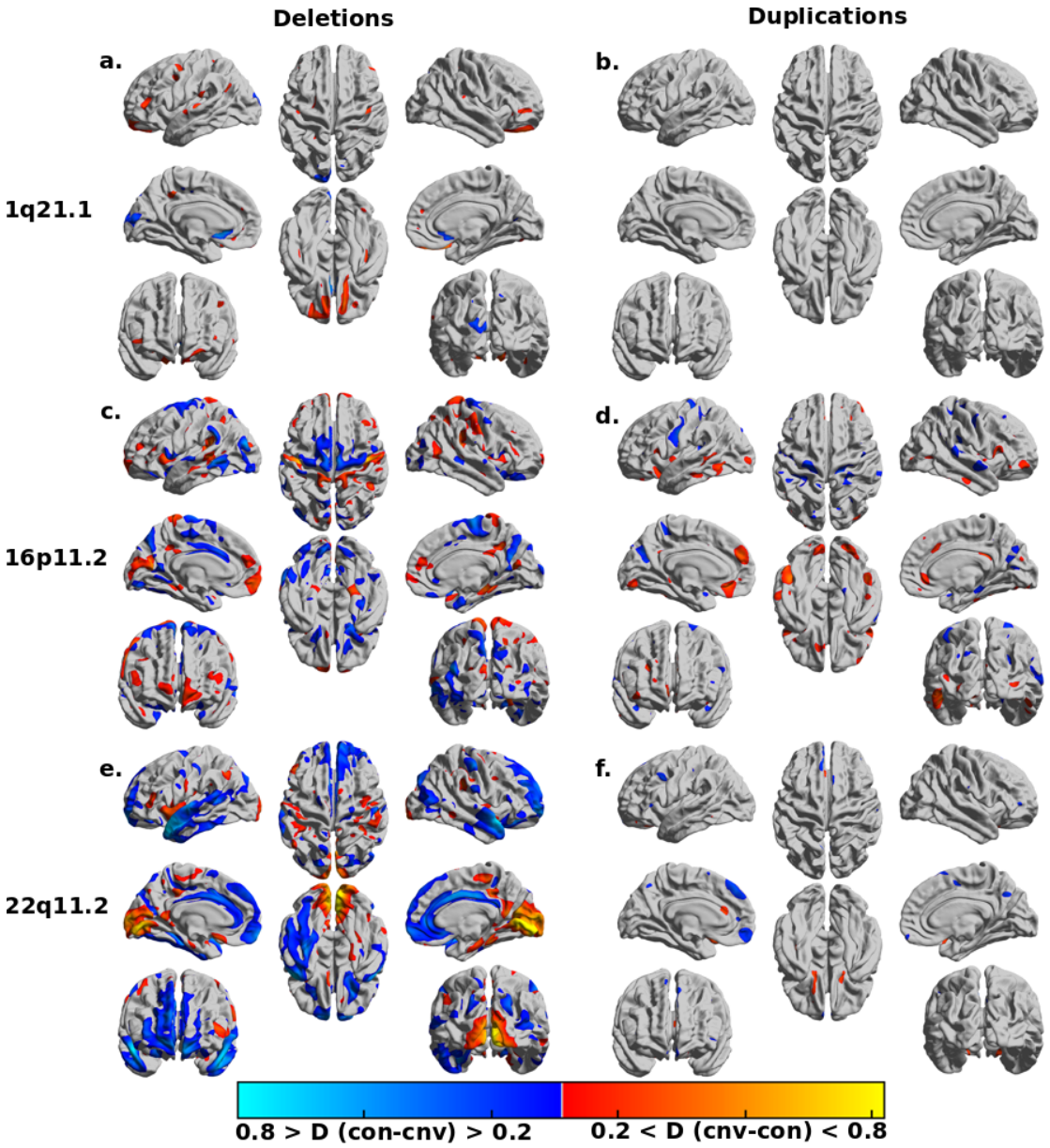

eFigure 4: FDR corrected Cohen's d maps of Cortical Thickness.

Legend: Vertex-wise brain differences in deletion and duplication carriers at the 1q21.1, 16p11.2 and 22q11.2. loci. 15q11.2 was not displayed because few vertices survived FDR correction. Left column

shows vertex-wise brain differences for deletion carriers (a, c, e) while right columns show vertex-wise brain differences for duplication carriers (b, d, f). Cohen's d effect sizes were estimated in SurfStat using vertex-wise CT estimate maps obtained from Freesurfer. Linear model was adjusted for sex, linear and quadratic expansion of age and mean cortical thickness. The results are significant at the FDR threshold $q < 0.05$ and shown within a range of 0.2 and 0.8 for comparison across CNVs.

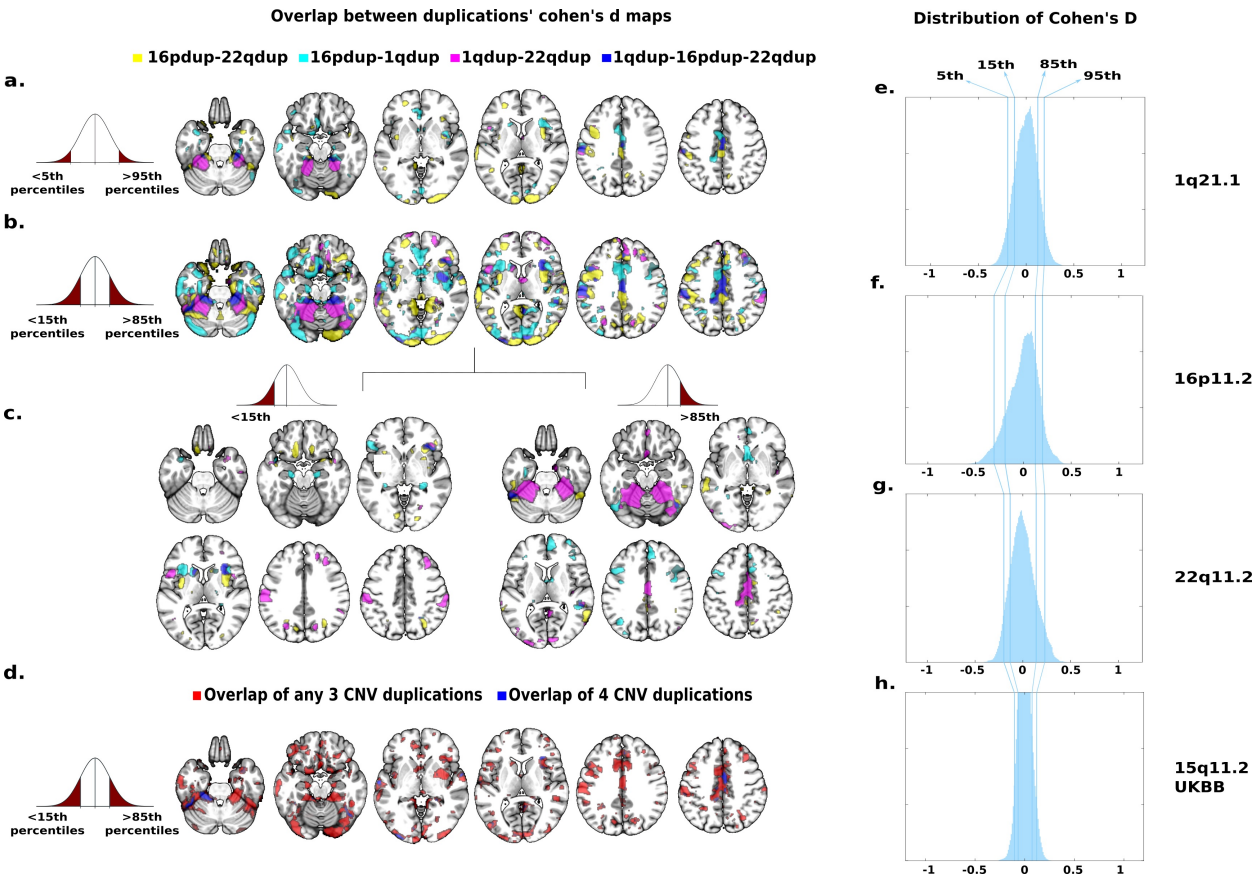

eFigure 5: Spatial overlap across duplications at 3 and 4 genomic loci

Legend: (a-c) The spatial overlap between the effects of 3 clinically ascertained duplications (16p11.2, 1q21.1 and 22q11.2) adjusted for effect size and sample size by using thresholds based on ranking : <5th and >95th (a), <15th and >85th percentile of Cohen's d values (b). Spatial overlap is shown separately for the top negative and positive Cohen's d values (c). Overlap across the 3 clinically ascertained deletions are reported in blue and pairwise overlaps are reported in purple, cyan and yellow. (d.) The spatial overlap across clinically and non-clinically ascertained duplications at 4 genomic loci for <15th and >85th percentile of Cohen's D values. Overlap of all four duplications is shown in blue. Overlap of any combination of three duplications is shown in red. Top ranking Cohen's D values used in (a, b, c, d) are presented on the density plots for all four duplications: 1q21.1 (e), 16p11.2 (f), 22q11.2 (g) and 15q11.2 (h). The X axes values of the 3 density plots are Cohen's d.

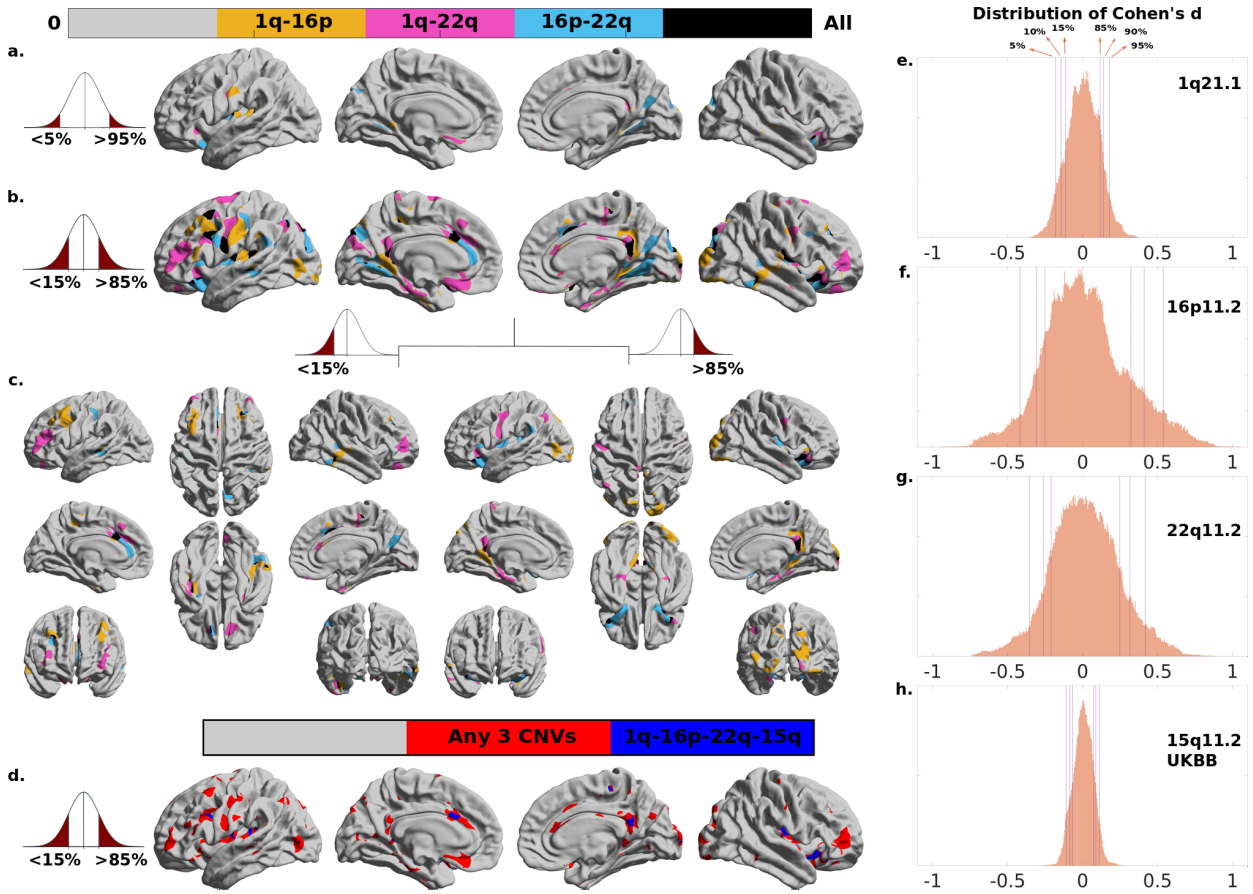

eFigure 6: Spatial overlap for surface area (SA) across deletions.

Legend: (a-c) The spatial overlap between the effects of 3 clinically ascertained deletions (16p11.2, 1q21.1 and 22q11.2), adjusted for effect size and sample size by using thresholds based on ranking: <5th and >95th (a), <15th and >85th percentile of Cohen's d values (b). Spatial overlap is shown separately for the top negative and positive Cohen's d values (c). Overlap across the 3 clinically ascertained deletions are reported in black and pairwise overlaps are reported in yellow, magenta, and cyan. (d.) The spatial

overlap across clinically and non-clinically ascertained deletions at 4 genomic loci for <15th and >85th percentile of Cohen's D values. Overlap of all four deletions is shown in blue. Overlap of any combination of three deletions is shown in red. Top ranking Cohen's d values used in (a-d) are presented on the density plots for all four deletions: 1q21.1 (e), 16p11.2 (f), 22q11.2 (g) and 15q11.2 (h). The X axes values of the 3 density plots are Cohen's d. (The conjunction of FDR corrected ($q < 0.05$) maps of 3 clinically ascertained deletions showed very few vertices and hence is not reported here).

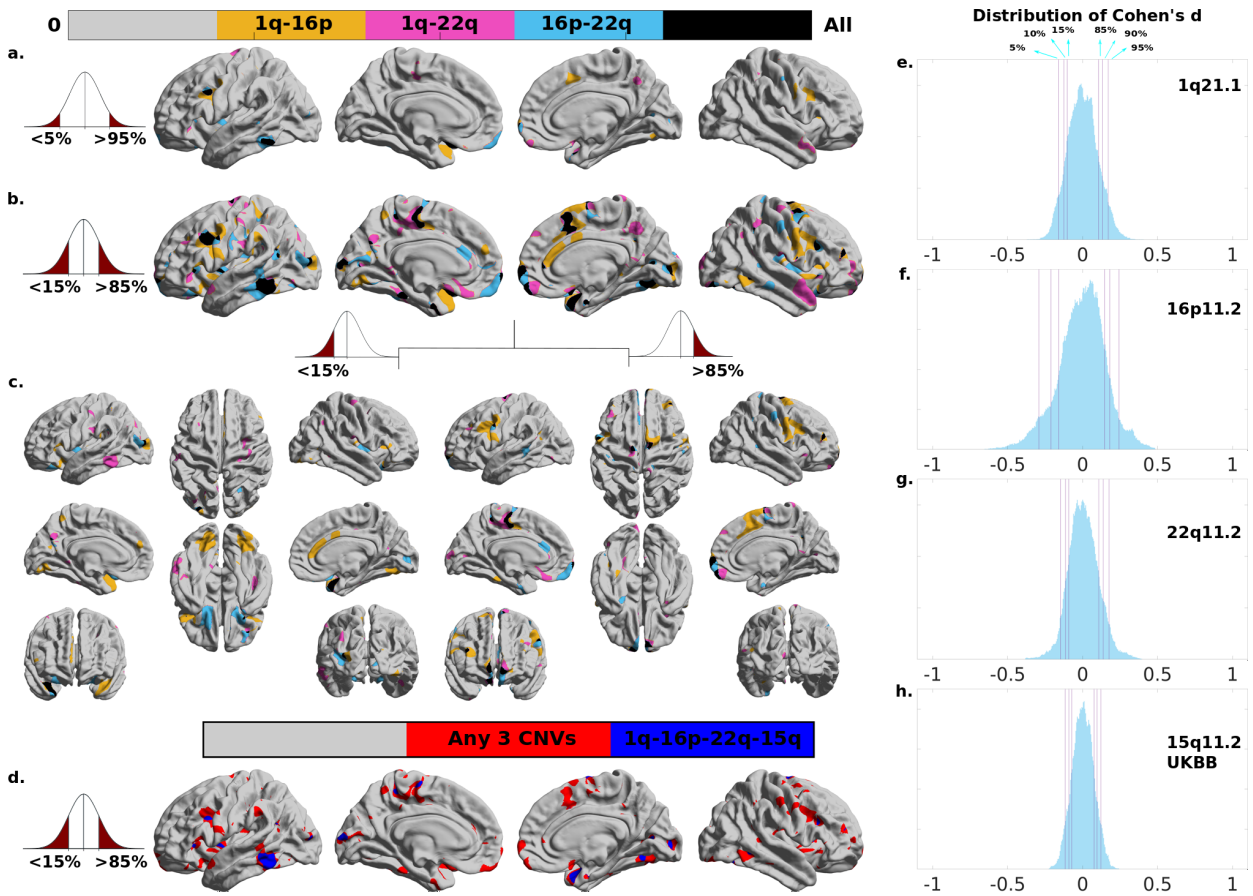

eFigure 7: Spatial overlap for surface area (SA) across duplications.

Legend: (a-c) The spatial overlap between the effects of 3 clinically ascertained duplications (16p11.2, 1q21.1 and 22q11.2), adjusted for effect size and sample size by using thresholds based on ranking: <5th and >95th (a), <15th and >85th percentile of Cohen's d values (b). Spatial overlap shown separately for the top negative and positive Cohen's d values (c). Overlap across the 3 clinically ascertained duplications are reported in black and pairwise overlaps are reported in yellow, magenta, and cyan. (d.) Spatial overlap across clinically and non-clinically ascertained duplication at 4 genomic loci for <15th and >85th percentile of Cohen's D values. Overlap of all four duplications is shown in blue. Overlap of any combination of three duplications is shown in red. Top ranking Cohen's d values used in (a-d) are presented on the density plots for all four duplications: 1q21.1 (e), 16p11.2 (f), 22q11.2 (g) and 15q11.2

(h). The X axes values of the 3 density plots are Cohen's d. (The conjunction of FDR corrected (q< 0.05) maps of 3 duplications showed no vertices and hence is not reported here).

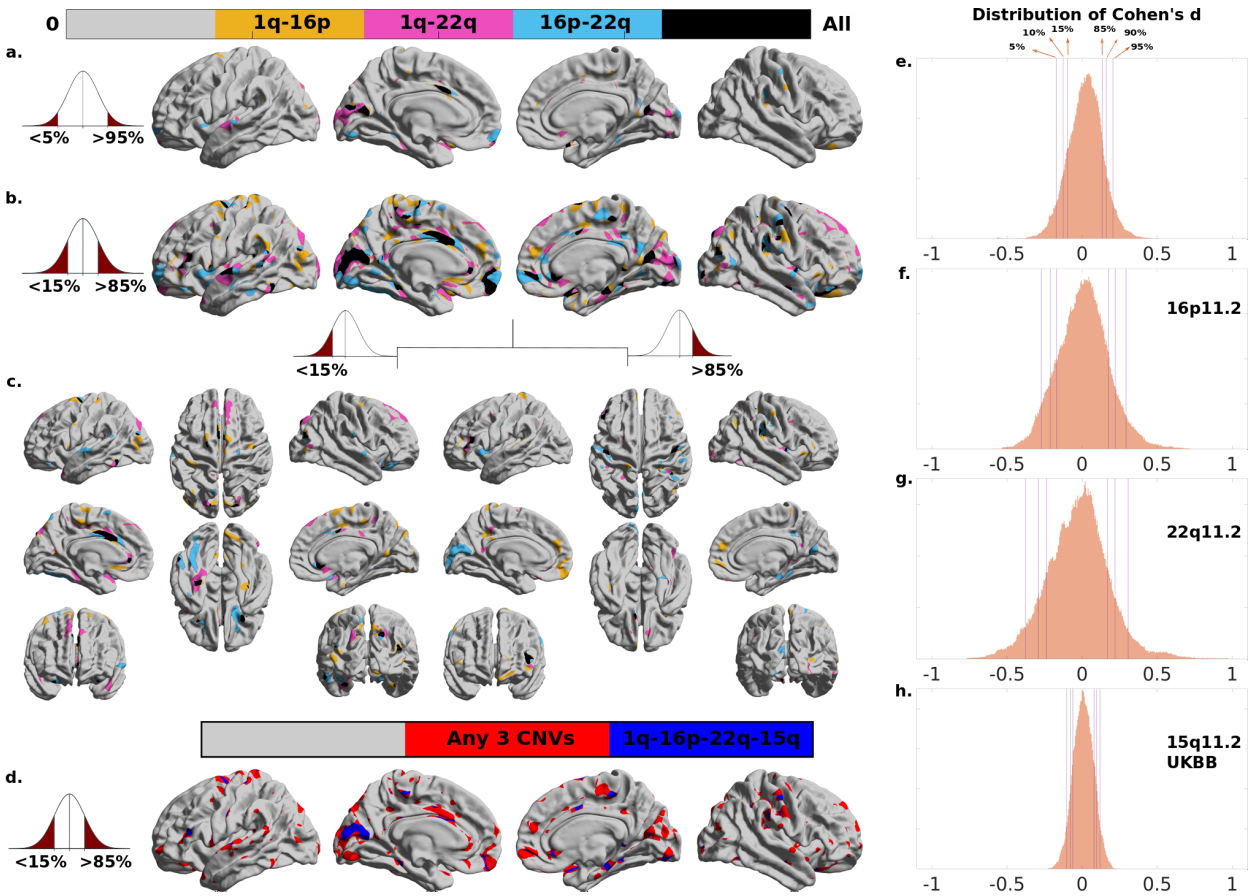

eFigure 8: Spatial overlap for mean cortical thickness (CT) across deletions.

Legend: (a-c) The spatial overlap between the effects of 3 clinically ascertained deletions (16p11.2, 1q21.1 and 22q11.2), adjusted for effect size and sample size by using thresholds based on ranking: <5th and >95th (a), <15th and >85th percentile of Cohen's d values (b). Spatial overlap is shown separately for the top negative and positive Cohen's d values (c). Overlap across the 3 clinically ascertained deletions

are reported in black and pairwise overlaps are reported in yellow, magenta, and cyan. (d.) Spatial overlap across clinically and non-clinically ascertained deletions at 4 genomic loci for the 15th and 85th percentile of Cohen's D values. Overlap of all four deletions is shown in blue. Overlap of any combination of three deletions is shown in red. Top ranking Cohen's d values used in (a-d) are presented on the density plots for all four deletions: 1q21.1 (e), 16p11.2 (f), 22q11.2 (g) and 15q11.2 (h). The X axes values of the 3 density plots are Cohen's d. (The conjunction of FDR corrected (q< 0.05) maps of 3 clinically ascertained deletions showed very few vertices and hence is not reported here).

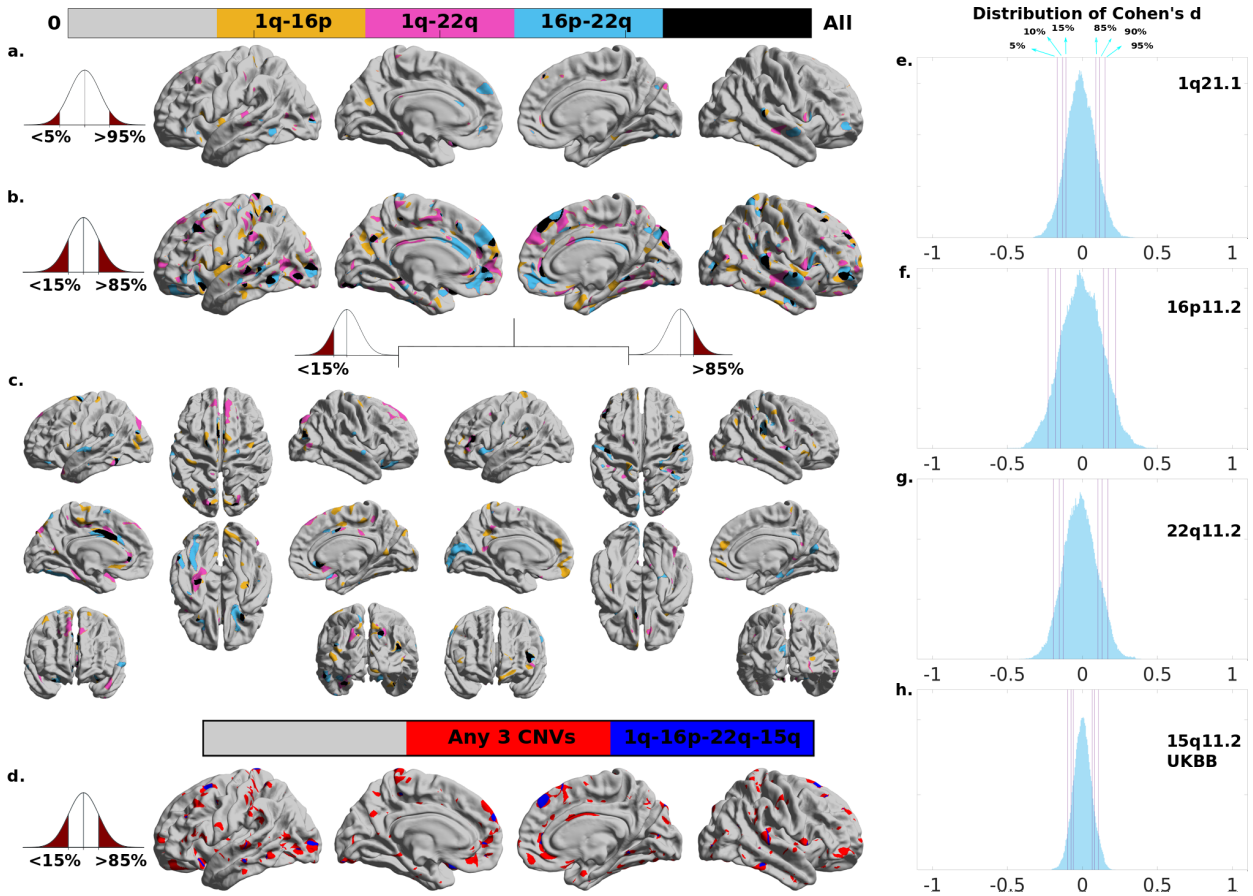

eFigure 9: Spatial overlap for mean cortical thickness (CT) across duplications.

Legend: (a-c) The spatial overlap between the effects of 3 clinically ascertained duplications (16p11.2, 1q21.1 and 22q11.2), adjusted for effect size and sample size by using thresholds based on ranking: <5th

and >95th (a), <15th and >85th percentile of Cohen's d values (b). Spatial overlap is shown separately for the top negative and positive Cohen's d values (c). Overlap across the 3 clinically ascertained duplications are reported in black and pairwise overlaps are reported in yellow, magenta, and cyan. (d.) Spatial overlap across clinically and non-clinically ascertained duplication at 4 genomic loci for <15th and >85th percentile of Cohen's D values. Overlap of all four duplications is shown in blue. Overlap of any combination of three duplications is shown in red. Top ranking Cohen's d values used in (a-d) are presented on the density plots for all four duplications: 1q21.1 (e), 16p11.2 (f), 22q11.2 (g) and 15q11.2 (h). The X axes values of the 3 density plots are Cohen's d. (The conjunction of FDR corrected ($q < 0.05$) maps of 3 duplications showed no vertices and hence is not reported here).

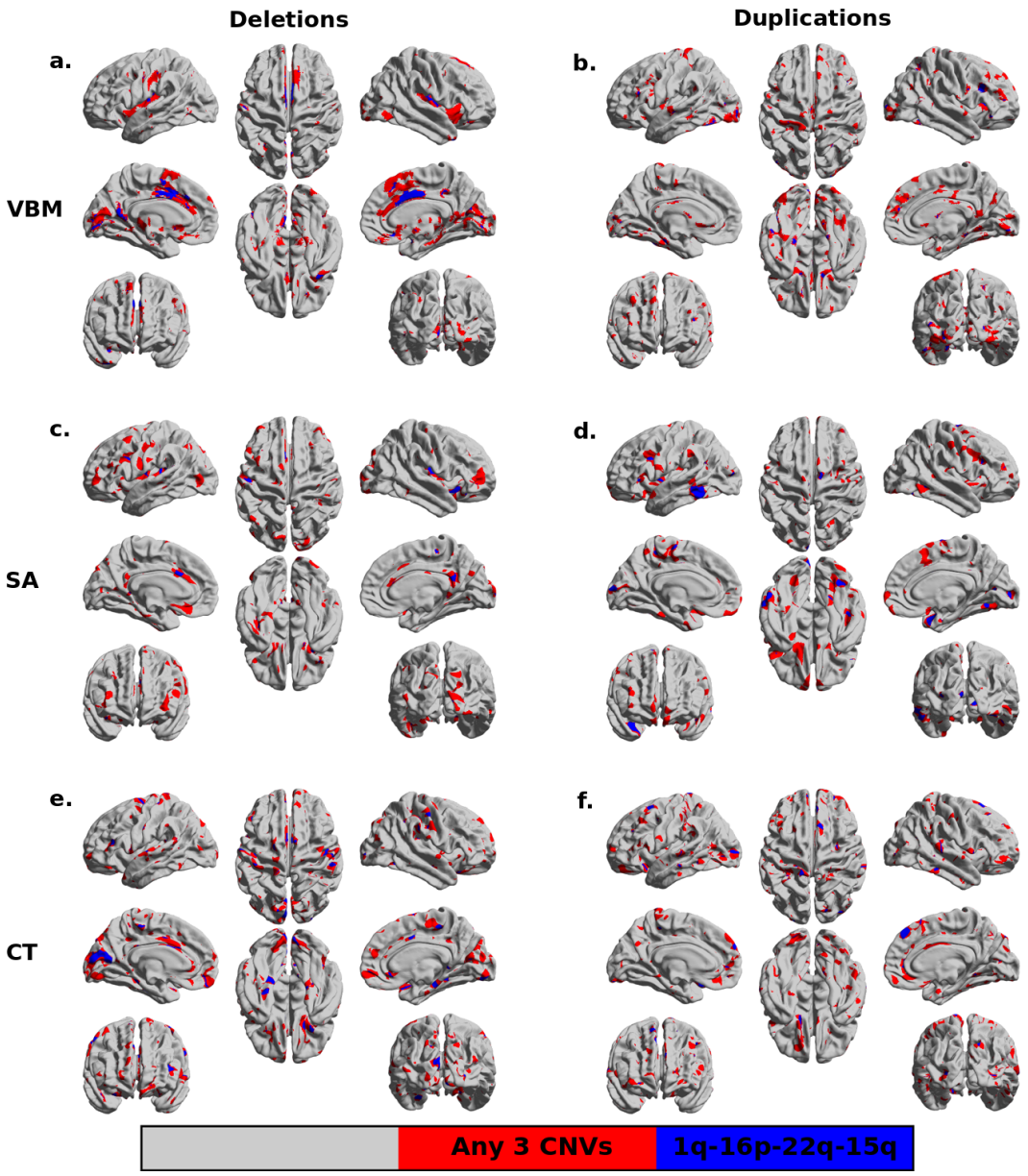

eFigure 10: Comparison of convergence patterns across brain measures.

Legend: Convergence patterns for 1q21.1, 16p11.2, 22q11.2, and 15q11.2 deletions (left) and duplications (right). Any 3 CNVs (red) and all 4 CNVs (blue) for: VBM (projected on fsaverage; a, b), Surface Area (c,d), and Cortical Thickness (e,f).

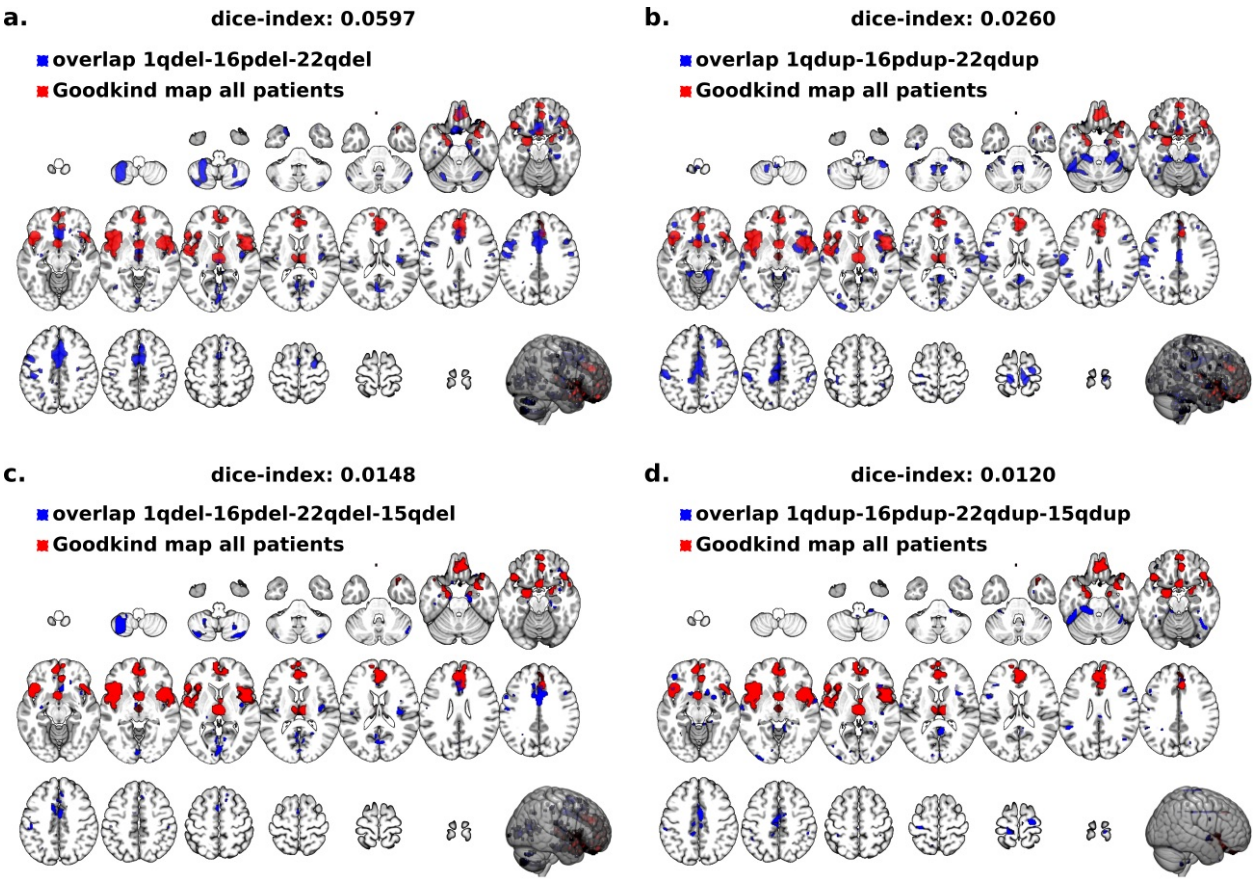

eFigure 11: Dice indices between cross-psychiatric disorder map and CNVs convergence patterns.

Legend: We computed dice indices between the cross-psychiatric disorder map published by Goodkind and colleagues (in red, Goodkind et al. 2015) and each CNVs convergence pattern (in blue): (a) overlap of 3 deletions, (b) overlap of 3 dupliations, (c) overlap of 4 deletions and (d) Overlap of 4 duplications.